



Exploring the impact resistance of hybrid sandwich composite body armor through experimental analysis



Waad A. Khalaf^{*}, Mohsin N. Hamzah^{ID}

Mechanical Engineering Dept., University of Technology-Iraq, Alsina'a street, 10066 Baghdad, Iraq.

*Corresponding author Email: mohsin.n.hamzah@uotechnology.edu.iq

HIGHLIGHTS

- The hybrid composite sandwich was carefully assembled with silicon adhesive bonding the core and skins.
- The composite skins were fabricated using the hand lamination technique.
- Authentic ballistic tests were conducted on the fabricated specimens.
- The refined design, sample (S3), effectively protected against penetration.
- Silicone rubber fillings have higher energy absorption compared with foam fillings.

ARTICLE INFO

Handling editor: Jalal M. Jalil

Keywords:

Ballistic Impact
7.62×39 mm bullet
Hybrid Sandwich Armor
Energy Absorption
Back Face Signature

ABSTRACT

Hybrid composite sandwich structures, known for remarkable energy absorption, rigidity, and strength, are emerging as a preferred choice for fortifying structures against a diverse range of firearms and artillery. Despite their higher density, these panels demonstrate commendable qualities, making them optimal for armored vehicles and body armor. Numerous structural options compete for recognition as effective ballistic shields in today's context. In this study, three sample configurations were rigorously tested for ballistic impact using a 7.62×39 mm bullet. The first sample (S1) comprised silicon carbide ceramic tiles (SiC), Kevlar fiber, and carbon fiber in the face sheet, with an unfilled aluminum honeycomb core and a carbon fiber rear sheet. Subsequent samples, S2 and S3, maintained the S1 composition but varied in the core. S2 had a honeycomb core injected with polyurethane foam, while S3 utilized a silicone rubber-filled honeycomb core. Ballistic tests revealed a notable difference: S1 and S2 failed to prevent bullet penetration, whereas S3 successfully met this crucial objective. After penetration, the bullets' velocities were S1 -45.9 m/s, S2-22.9 m/s, and S3 -0m/s. Remarkably, S3 exhibited an optimal 0mm back face signature (BFS) and a penetration depth (DOP) of 13.74 mm, well within limits. Cumulative energy absorption (EA) was as follows: S1-2577.23 J, S2-2583.57 J, and S3-2617.92 J. The armors demonstrated specific energy absorptions (SEA) of 2386.33, 2389.97, and 2015.32 J/kg, respectively. Their areal densities were 48, 48.1, and 57 kg/m², respectively. The ballistic limit velocities (BLV), derived from initial (IV) and residual velocities (RV), measured 802.68, 803.673, and 804 m/s for S1, S2, and S3.

1. Introduction

As military and paramilitary operations continually modernize, marked by technology-driven warfare and innovative ammunition tactics, an escalating demand for improved armor materials has emerged. These materials must be lighter, more damage-resistant, flexible, and capable of high energy absorption. This demand has driven the adoption of composite materials within armor systems. To effectively cater to the evolving needs of the armor industry, a comprehensive grasp of the scientific principles underpinning the design of sandwich armor structures becomes imperative. While a significant body of research has been dedicated to understanding armor fabrics and composites principles, the industry continues to grapple with critical challenges, particularly in mobility and protection. In armor materials, the primary requirements are mobility and protection. Balancing these two demands presents a complex scenario. Ballistic armors necessitate lightweight materials to ensure mobility, yet this runs contrary to the fact that enhanced protective properties often come with increased material weight, which can hinder mobility. Contemporary research focuses on reducing armor weight and enhancing its strength to optimize mobility and conserve energy for users.

Consequently, the field is increasingly drawn towards materials that are lightweight, flexible, and capable of high energy absorption. The emergence of sandwich composites has brought renewed attention due to their lightweight structure and high stiffness. The ability to choose from a wide array of reinforcing materials and the advancement of innovative processing

techniques further bolster the appeal of composite materials, opening doors to large-scale production [1]. Recently, extensive research endeavors have been dedicated to enhancing the performance of composite structures. Scholars are investigating a range of parameters of sandwich composite materials, strategically blending diverse constituents to amplify energy absorption capacities, all while maintaining a keen awareness of the structures' overall weight. Manipulating factors such as material attributes, thickness, and core properties contributes to fine-tuning the efficacy of sandwich composite structures. Incorporating cutting-edge materials in armor system production has notably bolstered the effectiveness of ballistic protection [2].

Numerous research studies have evaluated ballistic resistance within metallic and composite sandwich structures. The aim is to uncover material properties and assess their effectiveness when subjected to impact loads. For instance, Nia et al. [3] explored the mitigation of ballistic impact from blunt-nose rigid steel cylindrical projectiles using manufactured metallic honeycombs. The experimental tests utilized aluminum 5052-H39 honeycombs and were juxtaposed with analytical methodologies, revealing a minor discrepancy of approximately 10%. The outcomes unveiled a circular damage pattern on the front panel, while the rear exhibited an elliptical damage zone. This investigation contributes to our understanding of impact behavior in such structures.

In a study by Yang et al. [4], an innovative approach was introduced using an auxetic-honeycomb cored sandwich panel (AXP) for countering high-energy projectile impacts. The efficiency of this system was evaluated against an aluminum foam-cored sandwich panel (AFP) of identical density and dimensions. Employing numerical simulations, both panels were impacted, revealing the AXP's superior ballistic resistance attributed to its material concentration. Qi et al. [5] also explored honeycomb sandwich panels (HSPs) to solve ballistic trauma. Their sandwich panel comprised an aluminum alloy face sheet with three cell shapes (regular, rectangular, and hexagonal) within the honeycomb core. Numerical analysis involved impact simulations with spherical, conical, and blunt nose shapes. The findings highlighted increased residual velocity for blunter noses post-penetration of the honeycomb sandwich panels, showcasing its potential as an armor solution. Bhat [6] introduced a hybrid composite armor (HCA) with an aluminum honeycomb core to withstand high-energy projectiles at NIJ level III. A comparative analysis was conducted between the HCA system and the baseline (UHMWPE-Dyneema) HB50 fabric. The HCA system was constructed using HB50 fabric on the front face, an aluminum honeycomb core, and a thin HB50 layer. Experimental and numerical investigations demonstrated the HCA system's enhanced energy absorption, resulting in reduced weight and minimized behind-armor blunt trauma (BABT) compared to the baseline system.

In a study by Guo et al. [7], two armor configurations were numerically modeled. The first setup featured a dual-layer design with a ceramic plate on the front and a composite material (Kevlar-29) on the rear. In contrast, the second configuration replaced the ceramic plate with a ceramic-filled honeycomb in the back. Projectile impacts were applied to these panels, highlighting the significance of the ceramic honeycomb in effectively resisting high-energy impacts, especially those involving multiple hits.

In another investigation by Wang et al. [8], six honeycomb structure models were proposed, including square, triangle, reentrant, hexagonal, and two circular variations: circular honeycomb in square arrangement (CS) and circular honeycomb in hexagonal arrangement (CH). The study revealed that reentrant, triangular, and square shapes exhibited inferior performance compared to the hexagonal honeycomb. Conversely, the circular types demonstrated a lower residual velocity than the hexagonal honeycomb, indicating improved ballistic performance relative to the hexagonal shape.

The existing literature predominantly focuses on evaluating metallic sandwich structures, neglecting a comprehensive exploration of composite sandwich structures, encompassing both metallic honeycomb cores and composite skins. This study aims to develop an innovative personal body armor design that balances high protection, reasonable weight, and affordability while ensuring wearer safety. We propose combining sandwich structures and laminates (hybrid sandwich composite structure) to enhance ballistic performance, reduce behind-armor blunt trauma (BABT), and withstand multi-hit threats. This novel hybrid sandwich composite structure integrates an aluminum honeycomb core with ceramic tiles, reinforced polymers using Kevlar and carbon fibers as skins, and varied fillings within the honeycomb cells. The hybrid sandwich composite panels, comprising carbon fibers, Kevlar fibers, silicon carbide ceramic tiles, and aluminum honeycomb, are manufactured employing the hand lamination technique for the skins and water jet machine cutting for the aluminum honeycomb core. This innovative approach bridges the gap in research and extends the understanding of hybrid sandwich configurations.

2. Experimental part

2.1 Materials used

The first step in experimental work is to choose suitable materials for work. The materials used in the manufacturing process for the present work are listed below and shown in Figure 1. This Figure shows the main armor's materials used, where Figure 1a shows the aluminum honeycomb core, Figure 1b displays the silicon carbide (SiC) tiles, Figure 1c showcases the carbon fibers, Figure 1d presents the Kevlar fiber layers, Figure 1e features the epoxy resin, Figure 1f highlights the Silicon rubber filling, Figure 1g shows the Foam filling, and Figure 1h displays the MS hybrid polymer silicon adhesive.

- 1) Aluminum honeycomb: Many important characteristics are available in 3003 aluminum honeycomb; lightweight, high energy absorption, high stiffness, ductility, and compressibility ability. Hence, the aluminum honeycomb is used as a core to damp and absorb the remaining kinetic energy of the bullet after being impacted with ceramic tiles and fibers.
- 2) Silicon Carbide Ceramic Tiles (SiC): The ceramic material is one of the widely used materials in many armor applications due to its important characteristics. Therefore, the ceramic is used as a strike front sheet to erode, deform the projectile, and absorb the majority of the kinetic energy. Furthermore, the study selected this material for the following reasons: Medium-weight material, high compressive strength, and high hardness.

- 3) Composite material (woven Kevlar fiber, carbon fiber woven, and Epoxy resin): Kevlar and carbon considered as most solid organic materials widely used in armor systems. They have a high level of protection with the ability to fend off bullets and shrapnel. Therefore, the woven fabrics Kevlar and carbon are used as a front and back sheet to catch and absorb the remaining kinetic energy of the bullet after impacting with ceramic tiles. Moreover, the study selected these materials for the following reasons: High-strength strength, low areal density, suitable cost, comfortable for the body, high stiffness, and high elastic modulus.
- 4) MS hybrid polymer silicon: many important characteristics are available in modified-silane hybrid polymer: High tensile strength, high Shear strength, good flexibility and cure speed from 3-24 hours.
- 5) Filling materials (polyurethane foam and silicon rubber): Room-temperature-vulcanizing (RTV) silicone rubber and polyurethane (PU) foam are both thermosetting polymers. They are typically processed in liquid form, and then begin internal cross-linking as the material cools within a mold. This ultimately causes the material to set (harden). Many important characteristics are available in RTV silicone rubber: High energy absorption, excellent thermal resistance, and light viscosity. Also, the characteristics of PU foam are high energy absorption, low density, and abrasion resistance. Hence, the RTV silicon rubber and PU foam are used as reinforcing filling material inside the honeycomb core to strengthen the honeycomb core structure, delay the process of penetration, and prevent damage merging.

The Aluminum honeycomb was purchased from "Huarui Honeycomb Technology Co., Ltd, China". The ceramic tiles of silicon carbide (SiC) were purchased from "Ningxia Northern Hi-Tech Industry Co., Ltd., China ."The woven Kevlar (aramid) and woven Carbon fiber were supported by "Wuxi GDE Technology Co., Ltd. China ."Epoxy resin type (Sikadur 52LB) was purchased from Sikadur Company. MS hybrid polymer silicon was supported by Soudal company. The filling materials (polyurethane foam and silicon rubber) were supplied from the commercial market. Mechanical Properties of Woven fabric Kevlar and carbon [9], Aluminum alloy (AL3003) [10], Steel alloy 1080 [11], Ceramics Silicon Carbide, and Aluminum oxide (Al₂O₃) [12].

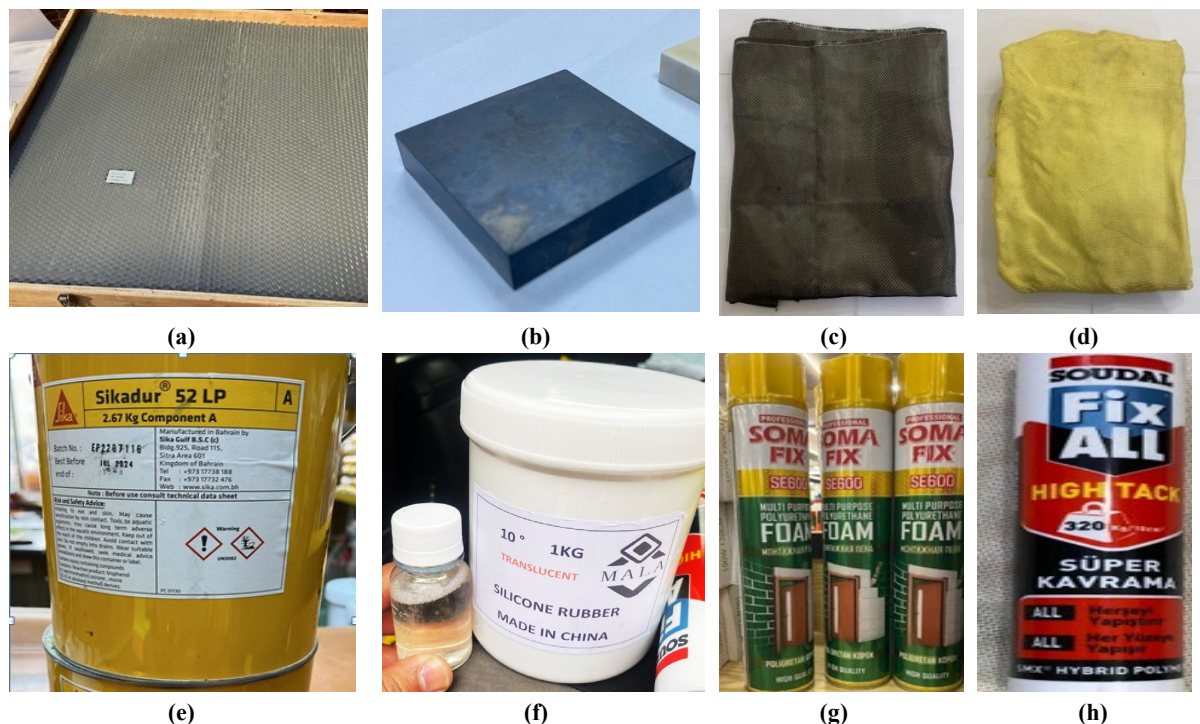


Figure 1: The main armor's materials used: (a) aluminum honeycomb core, (b) silicon carbide (SiC) tiles, (c) carbon fibers, (d) Kevlar fiber layers, (e) epoxy resin, (f) Silicon rubber filling, (g) Foam filling, and (h) MS hybrid polymer silicon adhesive

2.2 Composite Fabrication Process

The hand lay-up method is the open molding technique to fabricate composite material layers. This method has been used in the study to fabricate the composites consisting of a matrix material (epoxy) reinforced by layers of woven fabric of ballistic fibers Kevlar and carbon. First, cut the dry woven fabrics Kevlar and carbon according to the required dimensions (150 mm × 150 mm) by using a special cutter type due to the inability to cut these fibers by using traditional cutter types. After that, the mold was chosen as a glass sheet to provide a very fine surface finish with minimum defects to the composite layers. The mold was coated on the inner surface via a layer of wax to guarantee there was no adhesion between the composite material and the mold to facilitate the laminate removal. Then the base material of epoxy (resin) was mixed with the hardener taking into account that the weight percent between hardener and epoxy is 2:1.

After laying the first fiber layer, a layer of epoxy resin was added to the fiber layer and spread over the fiber with a brush. The next fiber layer was added to the first layer, and the resin was spread again. This process continued until all fiber layers were

laid on each other with the epoxy. To remove excess resin and bubbles in the resin, another glass sheet was laid on top of the laminated fibers, an appropriate load was used to squeeze the composite layers and the excess resin was allowed to escape from the sides. Finally, the skins were left to cure at room temperature for (24) hours before being extracted from the glass sheets. Figure 2 demonstrates the mold and fabrication process, with Figure 2a shows lay the first fiber layer, Figure 2b presents add layer of epoxy resin and (c) Figure 3c displays add the next fiber layer and spread the resin again. While Figure 3 showcases the final shape of the composite layers. Specifically, Figure 3a displays a Kevlar/Epoxy composite, and Figure 3b features a Carbon/Epoxy composite. These figures show the process of composite preparation and fabrication in the glass mold and the final shape of this composite after curing.

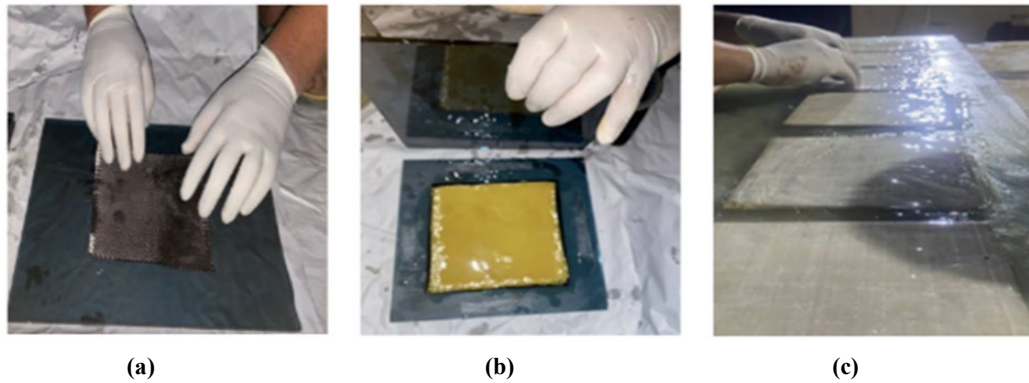


Figure 2: Mold Preparation and Fabrication Process: (a) Lay the first fiber layer, (b) Add layer of epoxy resin and (c) Add the next fiber layer and the resin was spread again

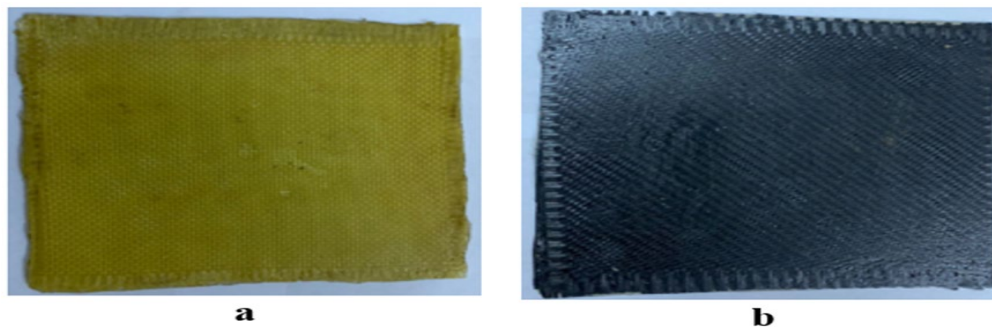


Figure 3: Final shape of composite layers: (a) Kevlar/Epoxy and (b) Carbon/Epoxy

2.3 Preparation of aluminum honeycomb

A water jet cutter machine was used to cut the al honeycomb structure to the required dimension (150×150 mm). This machine works depending on the principle of micro erosion, which occurs due to the large volume of the water jet through a very small-bore diameter of the nozzle (0.2 to 0.3 mm) with a very high jet speed, about 869 m/s with substantial kinetic energy. Figure 4 presents images of the machine, with Figure 4a highlighting the nozzle part and Figure 4b showcasing the control panel. The water jet cutting machine owns the main sub-systems, such as the water and abrasive tank. This high-pressure pump compresses water up to 3000 bar to generate sufficient kinetic energy for cutting, and high-pressure valves and a hydraulic unit. Figure 5 shows the final shape of the Aluminum honeycomb after cutting. To control the cutting process, this machine uses computer-aided manufacturing and design systems (CAD/CAM) [13].

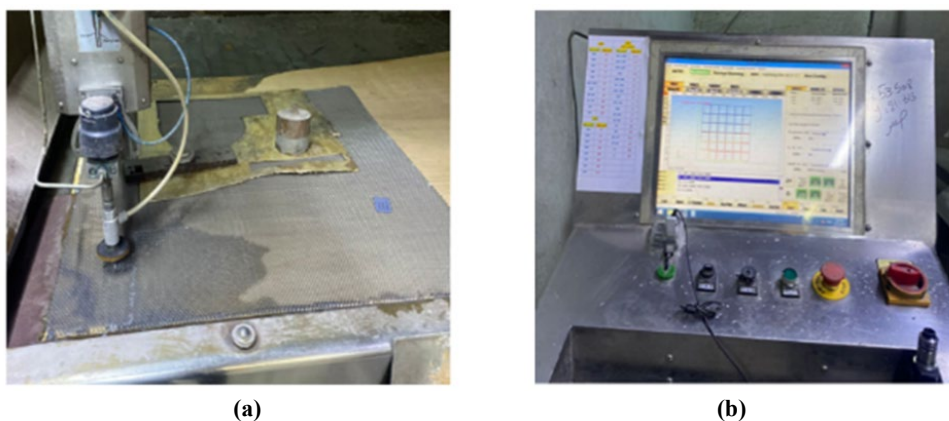


Figure 4: Water jet cutters (a) nozzle (b) computer

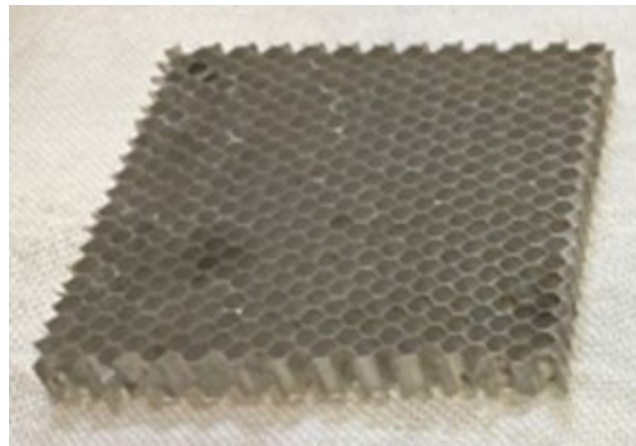


Figure 5: Final shape of Aluminum honeycomb after cutting

2.4 The layers assembly and fabrication of hybrid sandwich body armor

After completing the composite layers, the study prepared the sandwich structure body armor layers to be fabricated. The honeycomb core was assembled (glued) with the front and back sheets using the Modified-silane hybrid polymer silicon. It was left until full silicon curing of sandwich structure body armor samples. After completing the adhesive process, leave the sample at room temperature for 24 hours before using the samples in a ballistic test [14,15]. The MS hybrid polymer adhesive is excellent [16]. Figures 6-8 illustrate the assembly and fabrication of the hybrid sandwich body armor for Samples S1, S2, and S3, respectively. In each figure: (a) shows the schematic arrangement of layers; (b) presents the final isometric view; and (c) displays a photo of the finished armor. The three samples of hybrid sandwich body armor (150x150 mm²) were made. The first sample, S1, contains one layer of silicon carbide (SiC) and kevlar/epoxy and carbon/epoxy composite in the face sheets, the core includes unfilled honeycomb, and the back sheet contains carbon/epoxy composite. The second and third samples (S2 and S3) are similar to the first sample, but the difference is in the core, the honeycomb core with foam and silicone rubber filling, respectively. The cell size of the core is 6.4 mm for all samples. Table 1 provides the measurements and details of the various parts of the hybrid sandwich body armor.

Table 1: Details of hybrid sandwich body armor component (Three samples)

| Number of Sample | Face Skin material | Core material | Back Skin material | Thickness (mm) | | | core cell size (mm) | Armor Weight (g) | Armor Thickness (mm) | Notes |
|------------------|-------------------------|-----------------------|--------------------|----------------|------|-----------|---------------------|------------------|----------------------|-------------------------------|
| | | | | Face Skin | Core | Back Skin | | | | |
| 1 | SiC Kevlar carbon | Aluminum honeycomb | Carbon | 10 | 10 | 2 | 6.4 | 1079 | 30.4 | core without filling |
| | | | | 2 | | | | | | |
| | | | | 2 | | | | | | |
| 2 | SiC Kevlar carbon | Aluminum honeycomb | Carbon | 10 | 10 | 2 | 6.4 | 1082 | 29.6 | core with PU foam |
| | | | | 2 | | | | | | |
| | | | | 2 | | | | | | |
| 3 | SiC Kevlar carbon | Aluminum honeycomb | Carbon | 10 | 10 | 2 | 6.4 | 1283 | 29.3 | core with RTV silicone rubber |
| | | | | 2 | | | | | | |
| | | | | 2 | | | | | | |

2.5 Ballistic test: apparatus and test procurers

The chronograph term refers to an apparatus used to measure the speed of a projectile that is launched from any type of weapon or can be defined as a shooting speed tester. Consequently, this apparatus is one of the substantial tools used to characterize and assess any panel subject to the ballistic test [17]. The effective components of the apparatus are the photosensors and the light diffusers; thus, the accuracy of the chronograph completely depends on these components. The projectile's velocity is realized by dividing the distance between the two photosensors by the period between the projectile blocking the light in the first photosensor and blocking the light in the second photosensor. The perfect procedure of collecting data after accomplishing any ballistic test is important for the reliability of the test, and therefore this procedure must be completed carefully to obtain the required accurate results. Figure 9a shows the beta model chronograph that was used in this investigation. However, before implementing the ballistic test, the armor structure must be clamped using the backing material fixture. This equipment comprises several parts, such as a square frame, rigid plates, a hollow shaft, and the ground base [18]. The backing material fixture is constructed from a square frame. The front face of this frame is used to fix the armor structure by using rigid plates and bolts. Also, the back face of this frame can be closed or removed according to the kind of ballistic test. Indeed, the removable of the back face of the frame is applied for the perforation status, but this technique is not utilized for nonpenetrating panels. Figure 9b shows the equipment employed to achieve the ballistic test.

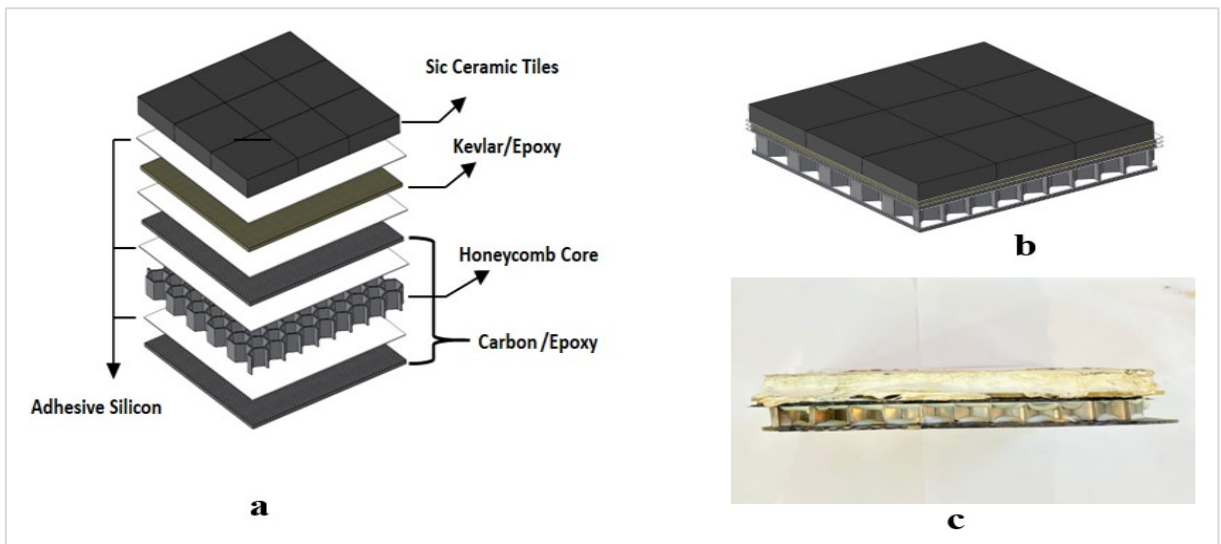


Figure 6: Sample S1 of the hybrid sandwich body armor (assembly and fabrication): (a) Schematic of arrangement of layers (b) Schematic of Isometric view (c) Photograph of Side view

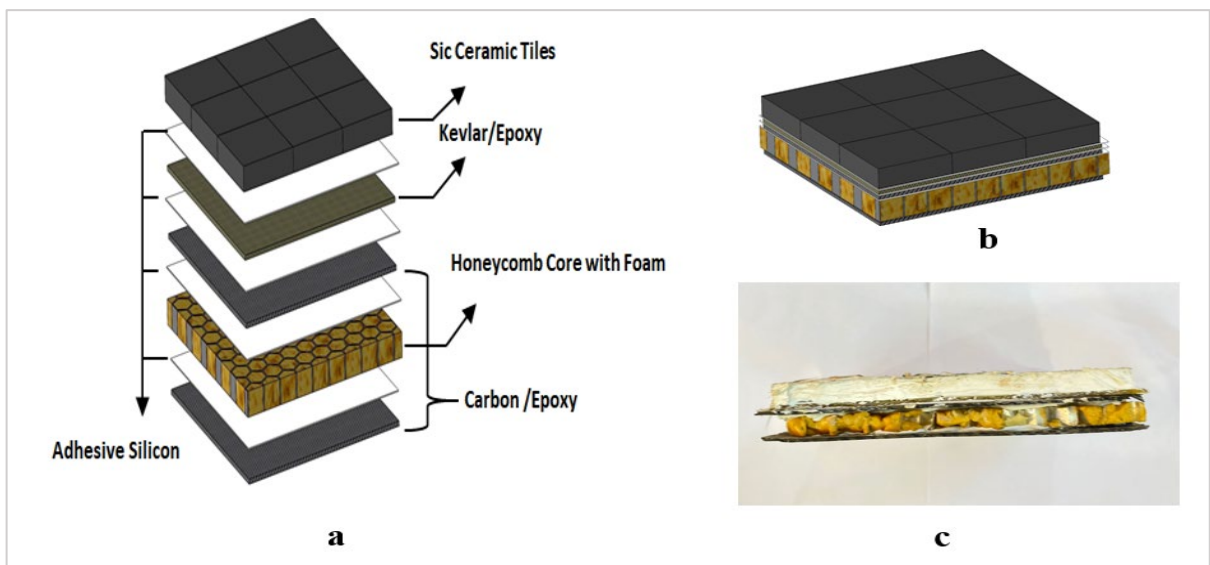


Figure 7: Hybrid sandwich body armor (second sample S2) after assembly and fabrication: (a) Schematic of arrangement of layers (b) Schematic of Isometric view (c) Photograph of Side view

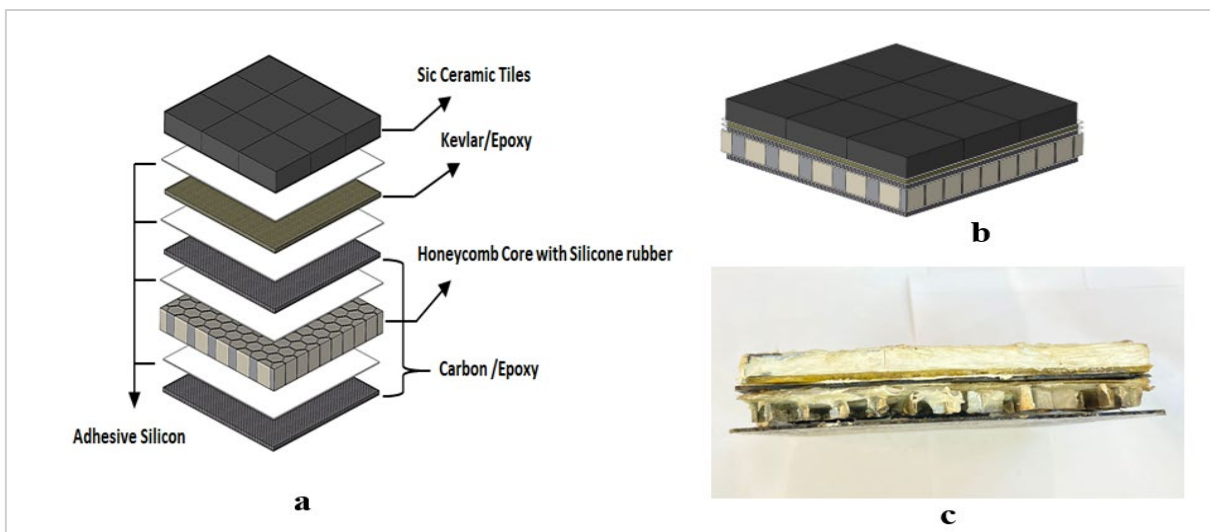


Figure 8: Hybrid sandwich body armor (third sample S3) after assembly and fabrication: (a) Schematic of arrangement of layers (b) Schematic of Isometric view (c) Photograph of Side view

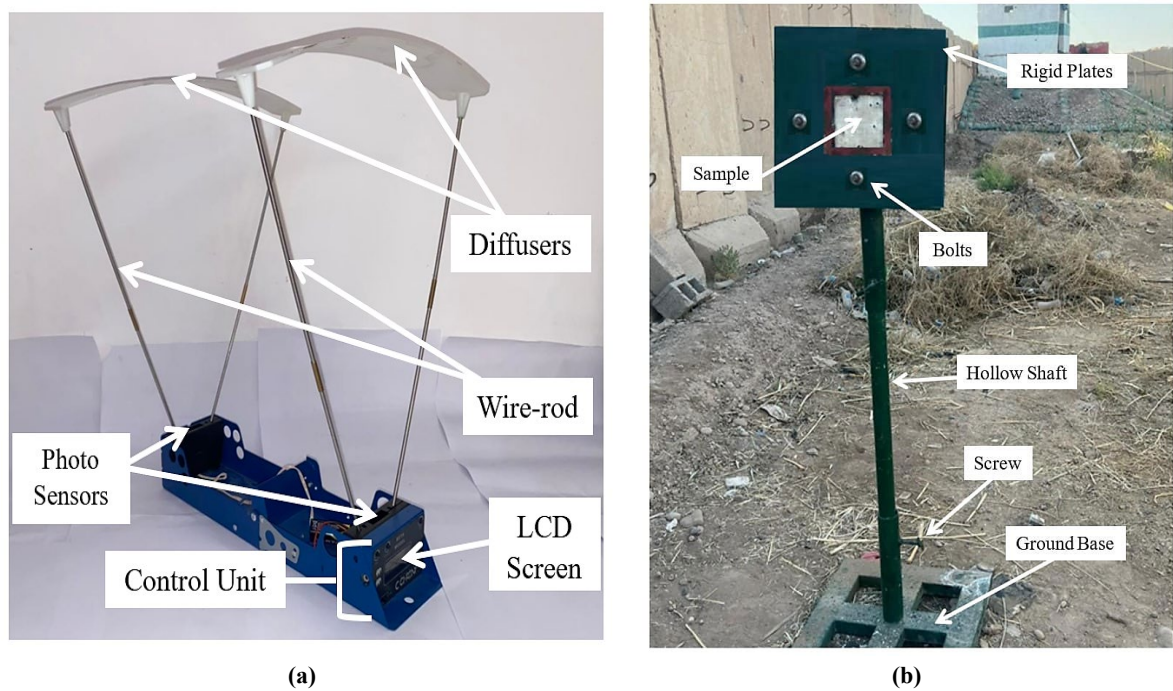


Figure 9: Schematics of the equipment and parts used in the final testing include: (a) a chronograph device and (b) abacking material fixture

To obtain a suitable ballistic response for an armor panel, it is necessary to acquire reliable data about the shots. Consequently, according to the National Institute of Justice (NIJ) ballistic standard, a particular number of shots are required for each round of tests [19]. Complete and partial penetration are the only two types of penetrations that exist for any impact test. Undoubtedly, the benefit from complete penetration is to calculate the energy absorption by the armor panel, and experimentally, that occurs when two devices of speed measurement are placed between the tested panel to measure the bullet speed before and after penetration. The initial or strike velocity and the residual velocity represent the velocities of the bullet before and after penetration, respectively. Hence, these velocities have been used to calculate the lost energy of the bullet [20].

Set up the distance between the muzzle and the backing material fixture; this distance equals (15.0 m ± 1.0 m). Set up the distance between the chronograph and the backing material fixture; this distance equals (2.5 m ± 25 mm). The test was done at a military base in Altaji belonging to the Iraqi popular mobilization forces in Baghdad, Iraq. Figure 10 offers the equipment for ballistic tests; all this equipment is set up according to the standard of NIJ.

2.6 The details of projectile

The bullet 7.62×39 mm is the projectile adopted in all study tests. This type of caliber is so familiar in this domain, and there are a large number of handguns that shoot this ammo. The weight of the bullet was 8g [21]. All specifications of the bullet have been included in Table 2.

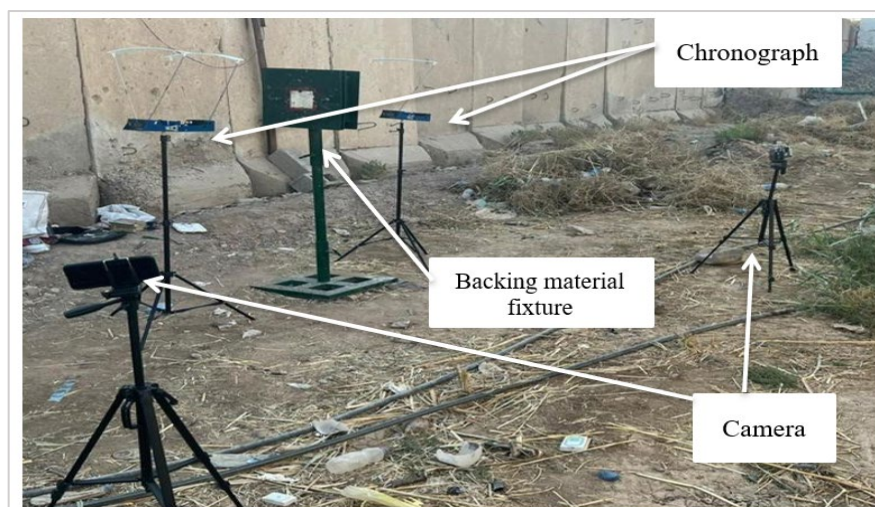


Figure 10: Photograph of the final ballistic test setup, showcasing the arrangement of the equipment utilized in this study

Table 2: Specifications of 7.62*39 mm bullet

| Caliber | Cartridge Weight (g) | Bullet Weight (g) | Bullet length (mm) | BulletDiameter (mm) | Cartridge Length (mm) |
|------------|----------------------|-------------------|--------------------|---------------------|-----------------------|
| 7.62×39 mm | 18 | 8 | 17.3 | 7.62 | 56 |

3. Results and discussion

This section presents the results of the ballistics tests performed on the manufactured hybrid sandwich armor specimens; these samples were classified based on the layers' protection, deformation, and order. Different materials are selected to fabricate the ballistic body armors: silicon carbide ceramic tiles 10 mm thickness, aluminum honeycomb 10 mm thickness; 6.4 mm cell size; carbon/ Epoxy 2 mm thickness and Kevlar/ Epoxy 2 mm thickness as well as a foam and silicone rubber as a filling material inside the aluminum honeycomb. Six parameters are used to analyze all samples after the impact of hybrid sandwich armor samples by the (7.62*39 mm) bullet under ballistic velocity impact (804 m/s). These parameters are the ability to withstand this projectile, layers order method, residual velocity, back face signature, the mode of deformation, and energy absorption.

Figures 11-13 show the deformation behavior of the hybrid sandwich composite body armors (HSCBA) in the real ballistic test for Samples S1, S2, and S3, respectively. In each figure: (a) shows the front face of the armor; (b) presents the back face signature; and (c) displays an isometric view of the armor. In the first sample (SiC, Kevlar/epoxy, carbon/epoxy, unfilled honeycomb core, and carbon/epoxy), the second and third samples are similar to the first. Still, the difference is in the core, with foam and silicone rubber filling for S2 and S3, respectively, knowing that the number of layers is equal in the face and the back sheets. Under the ballistic velocity impact, the HSCBA (S1 and S2) failed to stop the bullet, while the HSCBA S3 succeeded in stopping the bullet. The speeds of the bullet after penetration (RV) were (45.9, 22.9, and 0 m/s) for (S1, S2, and S3), respectively. HSCBA S3 regime made via the amalgamation of the strike of ceramic, Kevlar/epoxy as well as carbon/epoxy facing sheets, silicon rubber filled aluminum, the honeycomb core, and carbon/epoxy backing sheet demonstrated higher ballistic efficiency versus the kind (III) threat, utterly halting the projectile. From these figures, it can be seen that the armor samples (S1 and S2) failed to stop the bullet because of the absence of the reinforcing filling material of the honeycomb core structure in S1 and the weakness of the reinforcing filling material in the S2, as the use of foam filling in the second sample did not give sufficient reinforce compared to silicone rubber filling in the third sample, where S1 or S2 can be strengthened by filling the core with silicone rubber or increasing the number of layers to prevent the penetration. Also, the hybrid sandwich composite body armor S3 succeeded in stopping the bullet because of the filling of the aluminum honeycomb with silicone rubber.

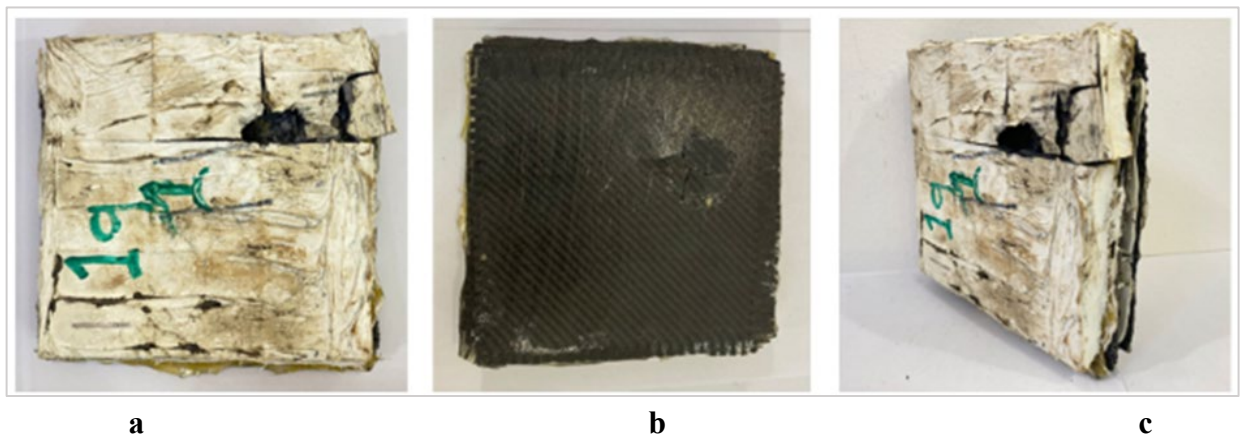


Figure 11: Photographs of the first sample (S21) post-ballistic impact, highlighting (a) the front face of the armor, (b) the back face signature, and (c) an isometric view of the armor

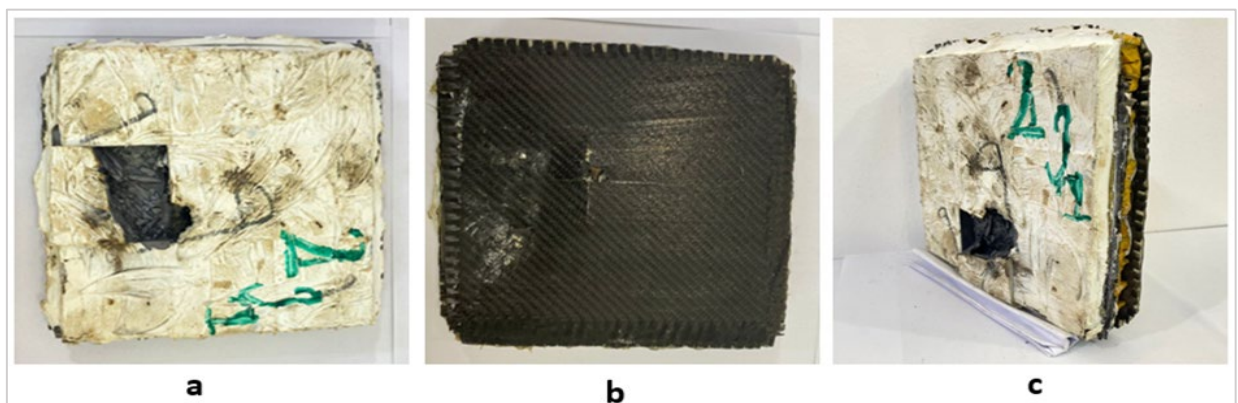


Figure 12: Photographs of the first sample (S22) post-ballistic impact, highlighting (a) the front face of the armor, (b) the back face signature, and (c) an isometric view of the armor

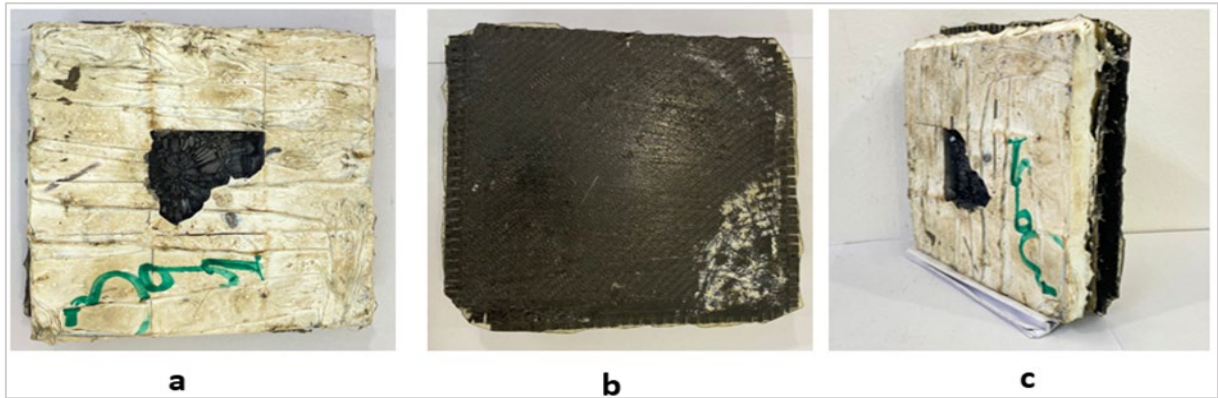


Figure 13: Photographs of the first sample (S23) post-ballistic impact, highlighting (a) the front face of the armor, (b) the back face signature, and (c) an isometric view of the armor

The S3 BFS was zero, which was optimum and in a permitted range [22]. And the DOP through this armor is (13.74) mm. Figure 14 shows the initial and residual velocity after the impact for the samples (S1, S2, and S3). It can be noticed the bullet can shatter the ceramics; this shattering is only in one tile in the bullet's impact zone and cracks in Kevlar/epoxy and carbon/epoxy layers, where the failure includes spalling, delamination, plastic deformation, and shearing failure. The numerous tile layouts have one advantage above a single ceramic layer: these tiles around the center are still in good condition and can withstand multiple impacts [23]. The aluminum honeycomb is lightweight but has poor ballistic ability when used as a single plate for protection. Still, it shows a good performance if layered with materials that have different properties and filled with reinforcing filling materials. This is attributed to the core structure, which helps compress and accumulate the cells under the projectile or the impact area of the projectile. The deformation of the aluminum in the honeycomb appeared to be ductile behavior after the ballistic impact and the fragmentation failure—the ceramic layer absorbed most of the projectile's kinetic energy through cracking and fracture. The face sheets contain a more significant number of layers compared to the back sheet, which enables the front sheets (fiber-reinforced composite) and aluminum the honeycomb to absorb the residual kinetic energy of projectile throughout the plastic deformation as well as the impairment and provide support for the cracked ceramic layer [24]. The back sheet was responsible for trapping and catching the fragments. The ceramic layer in the armors was for blunting, fracturing, or distorting the projectile [25]. Little projectile fragments stayed inside the carbon/epoxy. The core layers of honeycomb, or no projectile fragments, could be determined beyond the test NIJ-Kind (III) upon the armors [26], which proposes a comprehensive fragmentation of (7.62×39) bullet for the whole tested specimens. The bullet's kinetic energy represents the magnitude of the energy that the armor structure should absorb. Therefore, the kinetic energy undergoes a severe descent after impact, so the speed of the bullet after penetrating the armor is inversely proportional to the amount of absorbed energy. The initial or strike velocity and the residual velocity represent the velocities of the bullet before and after penetration, respectively. Hence, these velocities have been used to calculate the lost energy of the bullet and its specific via the Equations 1 and 2 [27,28]:

$$EA = \frac{1}{2} m (v_i^2 - v_r^2) \tag{1}$$

$$SEA = \frac{\Delta E}{m_s} \tag{2}$$

Vi and Vr represent the initial and residual velocities, m and ms represent the mass of the bullet and the mass of hybrid sandwich composite armor, and EA and SEA are the energy absorption and specific energy absorption, respectively, for the samples after the ballistic impact. After calculating the initial and residual velocity after the impact of the hybrid sandwich composite armors samples (S1, S2, and S3), calculate the value of the absorbed and the absorbed specific energy. Such armors' EA being (2577.23, 2583.56, and 2585.66) Joule, respectively, and the specific energy absorption of these armors is (2386.33, 2389.97, and 2015.32) Joule/kg, respectively. Figures 15 and 16 show the EA and SEA for every sample.

The term areal density is used to provide a consistent way of comparing the weights of armor. This is defined as the mass of armor per unit surface area, or it is found by multiplying the density of armor by the thickness and is usually stated in kg/m². The areal density of these armors samples (S1, S2, and S3) were 48, 48.1, and 57 kg/m², respectively. The ballistic limit velocity of the bullet represents the magnitude of the velocity required for a particular bullet to penetrate a particular piece of material reliably (at least 50% of the time). In other words, a given bullet will generally not pierce a given target when the bullet velocity is lower than the ballistic limit. The initial and residual velocities have been used to calculate the ballistic limit velocity of the bullet via the Equation 3 [29]:

$$v_b = \sqrt{v_i^2 - v_r^2} \tag{3}$$

Vi, Vr, and Vb represent the initial, residual, and ballistic limit velocities. After calculating the initial and residual velocity after the impact of the sandwich armors S1, S2, and S3, calculate the value of the ballistic limit velocity; therefore, the BLV

(calculated from IV and RV) of these armors were 802.68, 803.673, and 804 m/s, respectively. Figure 17 portrays the BLV versus the AD of hybrid sandwich composite armor samples. The results of this figure show that the whole penetration of S1 and S2 can be ascribed to the armor's low AD and every layer's premature failure. The results also show that using the silicone rubber filling in S3 results in a significant percent increase and improvement of the BLV and prevents penetration. This increase in sample AD coincides with this rise in BLV. These results indicate that by using the silicon rubber filling, the samples' ballistic resistance can be considerably improved, with a little rise in their AD. The relationship between EA and AD of the HSCBA samples is shown in Figure 18; also, the relationship between SEA and AD of HSCBA samples is shown in Figure 19. These figures demonstrate that adding silicon rubber filling to the S3 honeycomb core improves the SEA by a significant percentage. However, the sample areal density increase coincides with this increase in specific energy absorption. These results show that, with a slight increase in areal density, the samples' ability to absorb energy can be significantly improved by employing silicon rubber. Table 3 shows the results value of the ballistic test of IV, RV, BLV, AD, EA, SEA, DOP, and BFS of the hybrid sandwich composite armor samples. Suppose the comparison is made between the S1, S2, and S3. In that case, the S3 is stronger and could stop the bullet because the honeycomb was filled with silicone rubber, which postpones the penetration and avoids merging damage [25].

Table 3: The results of the experimental test of the HSCBA samples

| Sample | Initial velocity, IV (m/s) | Residual velocity (m/s) | Ballistic limit Velocity, BLV(m/s) | Areal density, AD(kg/m ²) | Energy absorption, EA (J) | Specific energy absorption, SEA(J/Kg) | BFS (mm) | DOP (mm) |
|--------|----------------------------|-------------------------|------------------------------------|---------------------------------------|---------------------------|---------------------------------------|----------|----------|
| S1 | 804 | 45.9 | 802.688 | 48 | 2577.23 | 2386.33 | - | - |
| S2 | 804 | 22.9 | 803.673 | 48.1 | 2583.56 | 2389.978 | - | - |
| S3 | 804 | 0 | 804 | 57 | 2585.66 | 2015.326 | 0 | 13.74 |

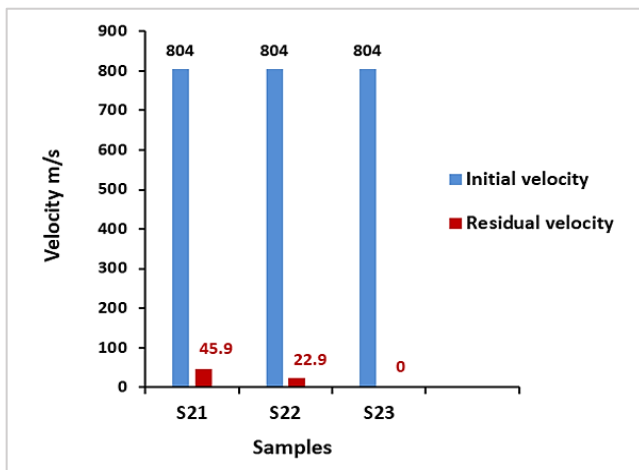


Figure 14: Initial velocity (IV) and residual velocity (RV) after the impact of the samples

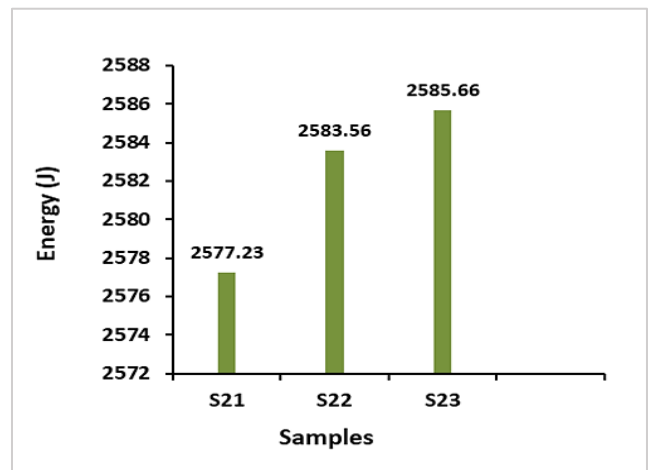


Figure 15: Energy absorption (EA) by each sample

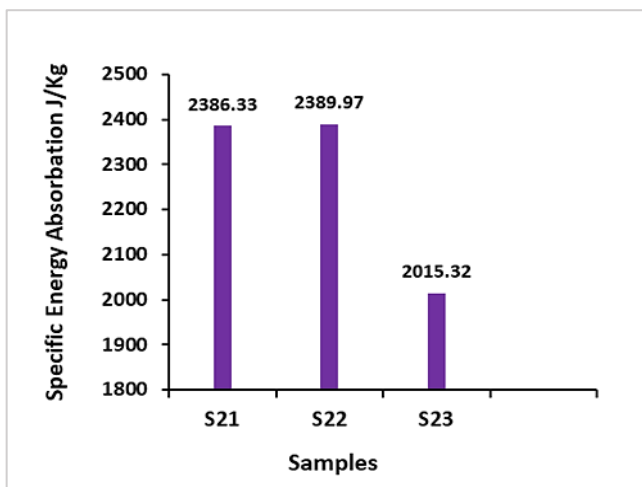


Figure 16: Specific energy absorption (SEA) by each sample

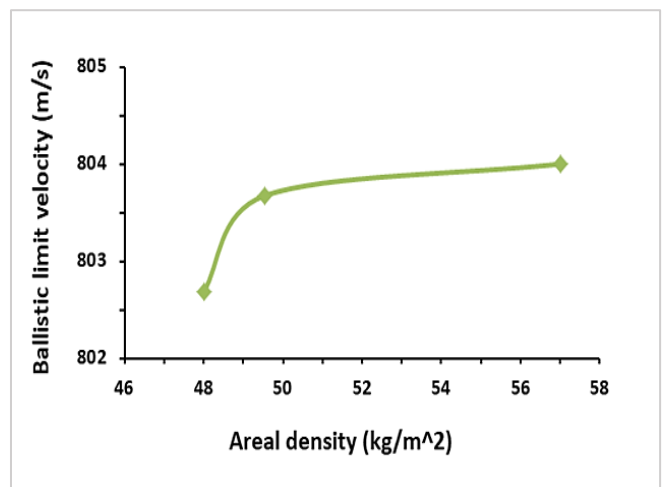


Figure 17: Relation between ballistic limit velocity (BLV) and areal density (AD) for all samples

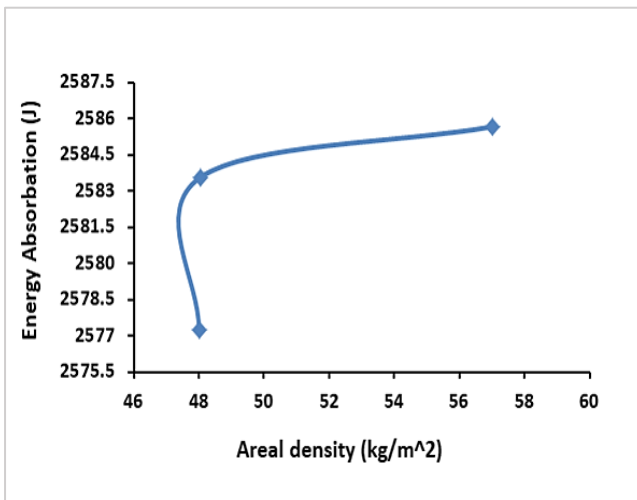


Figure 18: Relation between energy absorption (EA) and areal density (AD) for all samples

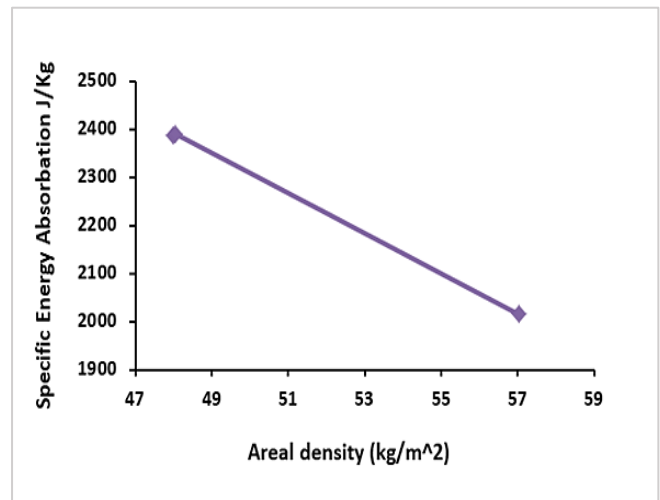


Figure 19: Relation between specific energy absorption (SEA) and areal density (AD) for all samples

4. Conclusion

The hybrid sandwich composite design's contribution focuses on accomplishing a prosperous and adaptive system that combines the appropriate weight and high protection. The hybrid sandwich composite design of body armor's ballistic impact with a 7.62×39 mm bullet provided the following significant essential points that highlight the significance of this structure:

- The analysis of the ballistic behavior of the hybrid sandwich composite armors shows the failure of these armors to absorb all the energy of impact except the S3 armor, which can withstand 7.62 mm ammunition and absorb all the energy of impact.
- The absorbed energy of these structures (hybrid sandwich composite armors) covered four levels of protection (IIA, II, IIIA, and III).
- After comparing the new body armor and the five levels of protection (IIA, II, IIIA, III, and IV), the new design can get armor with appropriate weight and high protection and fill the gap between these types.
- According to the deformation and damages of the hybrid sandwich composite body armors after the ballistic test, the comparison results between the hybrid sandwich composite body armors showed the S3 armor sample is the best armor in the ballistic tests where the S3 armor has the exceptional capability to absorb the impact's energy fully. In contrast, the S1 and S2 armors exhibited bullet penetration.
- The most noteworthy aspect is the achievement of a 0 mm back face signature by the S3 armor, emphasizing its efficacy in halting penetration.
- Additionally, the specific energy absorption corresponding to the initial impact velocity exhibited the following values for S1, S2, and S3: 2386.33, 2389.97, and 2015.32 Joule/kg, respectively. Furthermore, the areal densities of these armor samples were 48, 48.1, and 57 kg/m², respectively.

Abbreviations

| | |
|---------------|--|
| AD | Areal Density |
| BABT | behind armor blunt trauma |
| BFS | Back face signature |
| BLV | ballistic limit velocity |
| NIJ | National Institute of Justice |
| HSCBA | Honeycomb sandwich composite body armors |
| HSCBAs | Honeycomb sandwich composite body armors samples |
| SiC | Silicon Carbide |
| EA | energy absorption |
| SEA | Specific energy absorption |
| FRP | Fiber-reinforced polymer |
| IV | Initial velocity |
| RV | Residual velocity |
| RTV | room-temperature vulcanizing |
| PU | polyurethane |

Author contributions

Conceptualization, W. Khalaf and M. Hamzah; data curation, W. Khalaf and M. Hamzah.; formal analysis, W. Khalaf and M. Hamzah.; investigation, W. Khalaf and M. Hamzah.; methodology W. Khalaf and M. Hamzah.; project administration, W. Khalaf and M. Hamzah.; resources, W. Khalaf and M. Hamzah.; supervision, M. Hamzah.; validation, M. Hamzah.; visualization, W. Khalaf and M. Hamzah.; writing—original draft preparation, W. Khalaf and M. Hamzah.; writing—review and editing, W. Khalaf and M. Hamzah. All authors have read and agreed to the published version of the manuscript.

Funding

This research received no specific grant from any funding agency in the public, commercial, or not-for-profit sectors.

Data availability statement

The data supporting this study's findings are available on request from the corresponding author.

Conflicts of interest

The authors declare that there is no conflict of interest.

References

- [1] A. Ramanathan, P.K. Krishnan, R. Muraliraja, A review on the production of metal matrix composites through stir casting—Furnace design, properties, challenges, and research opportunities, *J. Manuf. Process.*, 42 (2019) 213-245. <https://doi.org/10.1016/j.jmapro.2019.04.017>
- [2] E. Medvedovski, Ballistic performance of armour ceramics: Influence of design and structure. Part 1, *Ceram. Int.*, 36 (2010) 2103-2115. <https://doi.org/10.1016/j.ceramint.2010.05.021>
- [3] A.A. Nia, S.B. Razavi, G.H. Majzoobi, Ballistic limit determination of aluminum honeycombs-experimental study, *Mater. Sci. Eng. A*, 488 (2008) 273-280. <https://doi.org/10.1016/j.msea.2007.11.044>
- [4] S. Yang, C. Qi, D. Wang, R. Gao, H. Hu, J. Shu, A comparative study of ballistic resistance of sandwich panels with aluminum foam and auxetic honeycomb cores, *Adv. Mech. Eng.*, 5 (2013) 589216.
- [5] C. Qi, S. Yang, D. Wang, L.J. Yang, Ballistic resistance of honeycomb sandwich panels under in-plane high-velocity impact, *Sci. World J.*, 2013 (2013) 20. <https://doi.org/10.1155/2013/892781>
- [6] Bhat, A. Honeycomb in hybrid composite armor resisting dynamic impact, Diss. Oklahoma State University, 2015. <https://hdl.handle.net/11244/299565>
- [7] G. Guo, S. Alam, L.D. Peel, Numerical analysis of ballistic impact performance of two ceramic-based armor structures, *Compos. C: Open Access*, 3 (2020) 100061. <https://doi.org/10.1016/j.jcomc.2020.100061>
- [8] Y. Wang, Y. Yu, C. Wang, G. Zhou, A. Karamoozian, On the out-of-plane ballistic performances of hexagonal, reentrant, square, triangular and circular honeycomb panels, *Int. J. Mech. Sci.*, 173 (2020) 105402. <https://doi.org/10.1016/j.ijmecsci.2019.105402>
- [9] O.H. Hassoon, M.S. Abed, J.K. Oleiwi, M. Tarfaoui, Experimental and numerical investigation of drop weight impact of aramid and UHMWPE reinforced epoxy, *J. Mech. Behav. Mater.*, 31 (2022) 71-82. <https://doi.org/10.1515/jmbm-2022-0008>
- [10] Y.B. Tan, X.M. Wang, M. Ma, J.X. Zhang, W.C. Liu, A study on microstructure and mechanical properties of AA 3003 aluminum alloy joints by underwater friction stir welding, *Mater. Charact.*, 127 (2017) 41-52. <https://doi.org/10.1016/j.matchar.2017.01.039>
- [11] A. Mishra, J. Maity, Structure–property correlation of AISI 1080 steel subjected to cyclic quenching treatment, *Mater. Sci. Eng. A*, 646 (2015) 169-181. <https://doi.org/10.1016/j.msea.2015.08.018>
- [12] J.F. Jiang, Y.F. Wu, Identification of material parameters for Drucker–Prager plasticity model for FRP confined circular concrete columns, *Int. J. Solids Struct.*, 49 (2012) 445–456. <https://doi.org/10.1016/j.ijsolstr.2011.10.002>
- [13] D.B. Rao, D. Baskey, R.S. Rawat, Water jet cutter: an efficient tool for composite product development, in Proceedings of the national conference on scientific achievements of SC & ST scientists & technologists, ational Aerospace Laboratories, Bangalore, 17, 2009, 104-107.
- [14] M.S. Al-Khazraji, S.H. Bakhy, M.J. Jweeg, Modal analysis of specific composite sandwich structures, *Eng. Technol. J.*, 41 (2023) 13-22. <http://dx.doi.org/10.30684/etj.2022.133585.1195>
- [15] I.A. Saleem, M.S. Abed, P.S. Ahmed, Numerical and Experimental Study of Hybrid Composite Body Armor, *Eng. Technol. J.*, 39 (2021) 1681-1687. <https://doi.org/10.30684/etj.v39i11.2274>

- [16] M.H. Mosa, M.N. Hamzah, Evaluating the Adhesive Properties of Four Types of Conventional Adhesives, *Eng. Technol. J.*, 40 (2022) 120-128. <https://doi.org/10.30684/etj.v40i1.2137>
- [17] W.K. Rule, S.E. Jones, A revised form for the Johnson–Cook strength model, *Int. J. Impact Eng.*, 21 (1998) 609-624. [https://doi.org/10.1016/S0734-743X\(97\)00081-X](https://doi.org/10.1016/S0734-743X(97)00081-X)
- [18] M.H. Mosa, M.N. Hamza, Influence of selection materials and construction techniques on the ballistic performance of armors: A review, *AIP Conf. Proc.*, 2404, 2021, 080025. <http://dx.doi.org/10.1063/5.0068916>
- [19] Y. Shin, J. Chung, J.H. Kim, Test and estimation of ballistic armor performance for recent naval ship structural materials, *Int. J. Nav. Archit. Ocean Eng.*, 10 (2018) 762-781. <https://doi.org/10.1016/j.ijnaoe.2017.10.007>
- [20] Rice, Kirk D., Michael A. Riley, and Amanda L. Forster, *Ballistic Resistance of Body Armor*, National Institute of Justice Office of Science and Technology Washington, 2008.
- [21] W. A. Khalaf and M. N. Hamzah, *Numerical Investigation of Impact Resistance of Honeycomb Composite Armor*, MESM, 2022.
- [22] National Institute of Justice, *Body Armor Guide: Selection & Application Guide 0101.06 to Ballistic-Resistant Body Armor*, 2014.
- [23] J. Marx, M. Portanova, A. Rabiei, Ballistic performance of composite metal foam against large caliber threats, *Compos. Struct.*, 225 (2019) 111032. <https://doi.org/10.1016/j.compstruct.2019.111032>
- [24] E. Medvedovski, Lightweight ceramic composite armour system, *Adv. Appl. Ceram.*, 105 (2006) 241–245. <http://dx.doi.org/10.1179/174367606X113537>
- [25] N.K. Naik, S. Kumar, D. Ratnaveer, M. Joshi, K. Akella, An energy-based model for ballistic impact analysis of ceramic-composite armors, *Int. J. Damage Mech.*, 22 (2013) 145–187. <https://doi.org/10.1177/1056789511435346>
- [26] M. Garcia-Avila, M. Portanova, A. Rabiei, Ballistic performance of composite metal foams, *Compos. Struct.*, 125 (2015) 202-211. <https://doi.org/10.1016/j.compstruct.2015.01.031>
- [27] S. Arora, A. Ghosh, Evolution of soft body armor, *Adv. Text. Eng. Mater.*, 7 (2018) 499-552. <https://doi.org/10.1002/9781119488101>
- [28] G. Sun, D. Chen, H. Wang, P.J. Hazell, Q. Li, High-velocity impact behaviour of aluminium honeycomb sandwich panels with different structural configurations, *Int. J. Impact Eng.*, 122 (2018) 119-136. <https://doi.org/10.1016/j.ijimpeng.2018.08.007>
- [29] R.F. Recht, T.W. Ipson, Ballistic perforation dynamics, *J. Appl. Mech.*, 30 (1963) 384-390. <https://doi.org/10.1115/1.3636566>